

# Measurements of the Vapor-Liquid Coexistence Curve in the Critical Region and the Critical Parameters of 1,1,2,2-Tetrafluoroethane

Jun Tatch, Shigeo Kuwabara,\* Haruki Sato, and Koichi Watanabe

Department of Mechanical Engineering, Faculty of Science and Technology, Keio University, 3-14-1 Hiyoshi, Kohoku-ku, Yokohama 223, Japan

The vapor-liquid coexistence curve in the critical region of 1,1,2,2-tetrafluoroethane (HFC-134) was measured by a visual observation of the meniscus in an optical cell. Eighteen saturated liquid densities and 10 saturated vapor densities have been obtained in a temperature range from 364 K to the critical temperature, corresponding to a density range from 243 to 1001 kg·m<sup>-3</sup>. The experimental uncertainties of temperature and density measurements are estimated to be within ±10 mK and between ±0.11% and ±0.44%, respectively. Not only the level where the meniscus disappeared but also the intensity of the critical opalescence was considered in the determination of the critical temperature and density being 391.74 ± 0.02 K (ITS-90) and 536 ± 2 kg·m<sup>-3</sup>, respectively. The critical exponent of the power law,  $\beta$ , was also determined as 0.347 ± 0.002. A saturated vapor-liquid density correlation has been developed on the basis of the present measurements.

## Introduction

We have consistently reported vapor-liquid coexistence curves and critical parameters of several CFC-alternative refrigerants: HFC-152a (1), HFC-134a (2), HCFC-123 (3), and HCFC-142b (4).

HFC-134 (1,1,2,2-tetrafluoroethane), which has no chlorine atom and then a zero ODP (ozone depletion potential) value, is one of the promising alternatives to replace CFC-12 (dichlorodifluoromethane) as a single refrigerant or one of the components of the binary refrigerant mixtures. This paper reports measurements of the vapor-liquid coexistence curve in the critical region, the experimentally-determined critical temperature, density, critical exponent of the power law,  $\beta$ , and a saturation density correlation of HFC-134.

## Experimental Section

An experimental apparatus used for all measurements has been reported by Okazaki et al. (5) who originally built it and Tanikawa et al. (3) who reconstructed it. The explanations of the apparatus and procedure have been reported in our previous publications (3, 5-7).

A standard platinum resistance thermometer, which was put in the vicinity of the optical cell in a thermostated fluid bath, was used for temperature measurements. The temperature values have been determined on two different temperature scales, IPTS-68 and ITS-90.

The experimental uncertainty of the temperature measurement is estimated to be within ±10 mK as a sum of ±2 mK for the accuracy of the thermometer, ±1 mK for the accuracy of a bridge, and ±7 mK for possible temperature fluctuation of silicone oil in the bath. The resistance value of the platinum resistance thermometer at the triple point of water was calibrated every half year. The resistance change of the thermometer was within ±0.0005% which corresponds to ±1.2 mK. The uncertainty of the density measurements is estimated to be between ±0.11%, which is considered to be due to the uncertainties of the determination of the cell volume and sample mass, and ±0.44%, which includes the uncertainty due to expansion procedures. Three different purity samples, 99.8 wt %, 99.983 mol %, and 99.94 mol %, were used in this study.

## Results

Saturated vapor densities were measured at temperatures above 382 K (0.975 at reduced temperature) and at densities between 243 (0.453 at reduced density) and 536 kg·m<sup>-3</sup> (critical density), whereas the saturated liquid densities were measured above 364 K (0.929) and between the critical density and 1001 kg·m<sup>-3</sup> (1.869). The experimental results including 10 saturated vapor densities and 18 saturated liquid densities are listed in Tables I and II.

Figure 1 shows the present results on a temperature-density diagram, together with the saturation densities at temperatures above 360 K measured by Maezawa et al. (8) and Tamatsu et al. (9). The present results of the saturated liquid densities agree with the measurements by Maezawa et al. (8) and Tamatsu et al. (9). But the measurements by Tamatsu et al. (9) show positive density deviations from the present results for saturated vapor and liquid densities.

Critical opalescence was observed for eight measurements at densities from 491.1 to 594.9 kg·m<sup>-3</sup>, corresponding to the temperatures below the critical temperature within 63 mK. The measurements when such critical opalescence was observed are given with an italic b in Tables I and II. For seven densities below 447.4 kg·m<sup>-3</sup>, the meniscus descended with increasing temperature and disappeared at the bottom of the optical cell. For 13 densities above 627.5 kg·m<sup>-3</sup>, the meniscus ascended with increasing temperature and disappeared at the top of the optical cell. For the other eight densities near the critical density, the meniscus disappeared without reaching either the top or bottom of the optical cell. The critical opalescence was observed clearly and more intensely in the liquid phase, and the meniscus descended slightly when the average density of the sample fluid in the optical cell was 528.2 kg·m<sup>-3</sup>; this means that the critical density is larger than this average density.

The opalescence, on the other hand, was observed more intensely in the vapor phase, and the meniscus ascended slightly when the average density was 541.3 kg·m<sup>-3</sup>; this means that the critical density is lower than this average density. At 534.3 kg·m<sup>-3</sup>, the most intense opalescence was observed and the meniscus descended slightly before it disappeared. Hence, we considered that the density of 534.3 kg·m<sup>-3</sup> was a saturated vapor density but the closest density to the critical point among the measurements in the vapor phase. At 538.6 kg·m<sup>-3</sup>, on the other hand, the most intense opalescence was also

\* To whom correspondence should be addressed.

**Table I. Saturated Vapor Densities  $\rho''$  of HFC-134<sup>a</sup>**

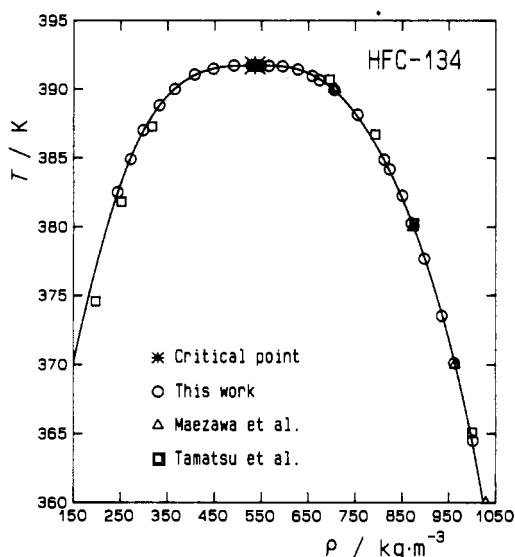
| $T_{90}/K$ ( $T_{68}/K$ ) | $\rho''/(kg\cdot m^{-3})$ | $T_{90}/K$ ( $T_{68}/K$ ) | $\rho''/(kg\cdot m^{-3})$ |
|---------------------------|---------------------------|---------------------------|---------------------------|
| 382.507 (382.536)         | 243.7 ± 1.1               | 391.083 (391.113)         | 407.3 ± 1.0               |
| 384.915 (384.943)         | 271.6 ± 1.1               | 391.495 (391.525)         | 447.4 ± 0.9               |
| 387.042 (387.072)         | 298.3 ± 1.1               | 391.743 (391.773)         | 491.1 ± 1.1 <sup>b</sup>  |
| 388.842 (388.872)         | 332.6 ± 1.1               | 391.741 (391.772)         | 528.2 ± 0.8 <sup>b</sup>  |
| 390.021 (390.051)         | 365.3 ± 1.0               | 391.760 (391.790)         | 534.3 ± 0.6 <sup>b</sup>  |

<sup>a</sup> Sample purity for all measurements was 99.94 mol %. <sup>b</sup> Critical opalescence was observed.

**Table II. Saturated Liquid Densities  $\rho'$  of HFC-134**

| $T_{90}/K$ ( $T_{68}/K$ ) | $\rho'/(kg\cdot m^{-3})$   | $T_{90}/K$ ( $T_{68}/K$ ) | $\rho'/(kg\cdot m^{-3})$  |
|---------------------------|----------------------------|---------------------------|---------------------------|
| 391.730 (391.760)         | 538.6 ± 0.9 <sup>a,b</sup> | 388.174 (388.204)         | 754.8 ± 0.7 <sup>d</sup>  |
| 391.739 (391.769)         | 541.3 ± 1.7 <sup>b,c</sup> | 384.887 (384.916)         | 811.9 ± 1.3 <sup>a</sup>  |
| 391.718 (391.748)         | 547.9 ± 0.6 <sup>a,b</sup> | 384.175 (384.204)         | 823.7 ± 0.7 <sup>d</sup>  |
| 391.710 (391.740)         | 565.7 ± 0.6 <sup>a,b</sup> | 382.267 (382.295)         | 850.5 ± 0.8 <sup>c</sup>  |
| 391.675 (391.707)         | 594.9 ± 2.1 <sup>b,c</sup> | 380.270 (380.298)         | 869.8 ± 0.7 <sup>a</sup>  |
| 391.438 (391.468)         | 627.5 ± 0.7 <sup>a</sup>   | 377.690 (377.723)         | 897.7 ± 1.3 <sup>d</sup>  |
| 390.970 (391.000)         | 658.2 ± 1.3 <sup>d</sup>   | 373.550 (373.577)         | 935.0 ± 1.3 <sup>c</sup>  |
| 390.663 (390.693)         | 673.5 ± 1.1 <sup>d</sup>   | 370.137 (370.163)         | 961.7 ± 0.9 <sup>d</sup>  |
| 389.970 (390.000)         | 704.8 ± 1.0 <sup>d</sup>   | 364.500 (364.526)         | 1001.6 ± 0.9 <sup>c</sup> |

<sup>a</sup> Measurements with 99.94 mol % purity sample. <sup>b</sup> Critical opalescence was observed. <sup>c</sup> Measurements with 99.983 mol % purity sample. <sup>d</sup> Measurements with 99.8 wt % purity sample.

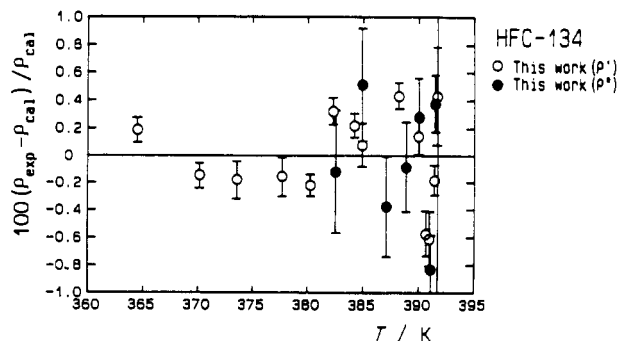
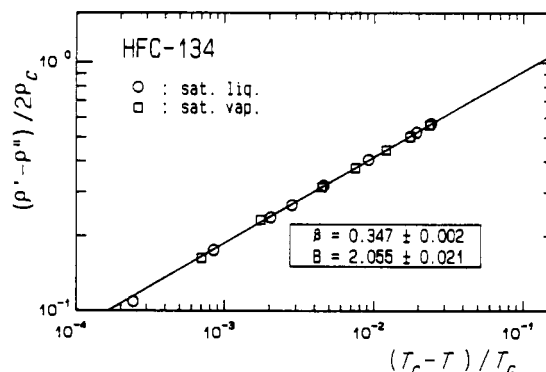
**Figure 1. Vapor-liquid coexistence curve of HFC-134.**

observed and the meniscus ascended slightly before it disappeared. We concluded therefore that the density of 538.6 kg·m<sup>-3</sup> was a saturated liquid density but the closest density to the critical one among the measurements in the liquid phase. Therefore, we surmised that the critical density should be in between these two density values. Thus, we determined the critical density of HFC-134 to be  $\rho_c = 536 \pm 2$  kg·m<sup>-3</sup>.

The critical temperature should be determined as the saturation temperature which corresponds to the critical density. Saturation temperatures of three vapor and five liquid densities associated with an italic b in Tables I and II were considered for the determination of the critical temperature. We determined the critical temperature of HFC-134 to be  $T_c = 391.77 \pm 0.02$  K (ITS-68),  $391.74 \pm 0.02$  K (ITS-90). The uncertainty of  $\pm 20$  mK consists of  $\pm 10$  mK for the uncertainty of temperature measurements and  $\pm 10$  mK for the possible difference due to individual judgements of the disappearance of the meniscus.

## Discussion

The critical exponent,  $\beta$ , is essential for modeling the vapor-liquid coexistence curve in the critical region by means of the

**Figure 2. Deviation of the saturated vapor and liquid densities from eq 2.****Figure 3. Determination of the critical exponent and amplitude.**

following power law representation:

$$(\rho' - \rho'')/2\rho_c = B[(T_c - T)/T_c]^\beta \quad (1)$$

where  $\rho_c$  is the critical density,  $T_c$  is the critical temperature, and the single prime and double prime denotes saturated liquid and vapor, respectively.  $B$  is the critical amplitude. Equation 1 requires isothermal pairs of liquid and vapor densities. Hence, we used the following correlation for the calculation of a pair of saturated liquid and vapor densities:

$$(\rho - \rho_c)/\rho_c = -13.099\tau^{1-\alpha} + 24.632\tau - 18.651\tau^{1-\alpha+\Delta_1} \pm 1.7983\tau^\beta \pm 0.62545\tau^{\beta+\Delta_1} \quad (2)$$

where  $\tau = (T_c - T)/T_c$ ,  $\alpha$  and  $\beta$  are critical exponents, and  $T$  is the temperature in Kelvin on ITS-90. The exponent  $\Delta_1$  stands for the first symmetric correction-to-scaling exponent of the Wegner expansion (10). From a theoretical background (10), these exponents were determined as follows:

$$\alpha = 0.1085 \quad \beta = 0.325 \quad \Delta_1 = 0.50$$

The coefficients in eq 2 were determined by the least-squares fitting to the present measurements, where seven densities between 491.1 and 565.7 kg·m<sup>-3</sup> around the critical point were not used. The upper sign "+" and lower "-" of the fourth and fifth terms in eq 2 correspond to the saturated liquid and vapor, respectively. The effective density range of eq 2 is between 243 and 1001 kg·m<sup>-3</sup>. The saturation curve calculated from eq 2 is shown in Figure 1. The density deviations of the input data from eq 2 are shown in Figure 2. The deviations of the saturated liquid densities are shown with open symbols, while those for the saturated vapor are shown with solid symbols in Figure 2. Equation 2 reproduces 14 present saturated liquid densities with the standard deviation of 0.28%. The maximum deviation among those of the present measurements was -0.8% near the critical density.

Figure 3 shows logarithmic plots in terms of the present measurements and calculated results from eq 2. The power

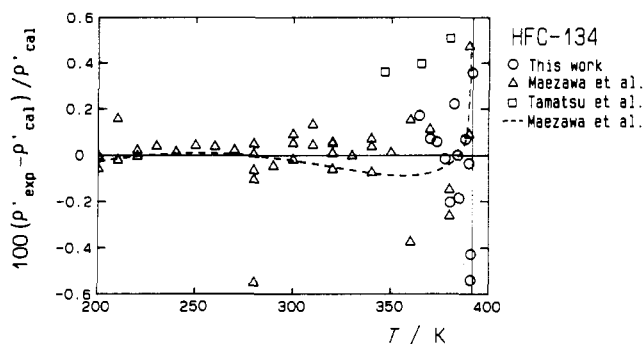


**Figure 4.** Deviations of the saturated liquid densities from eq 3.

law representation, eq 1, suggests that the present experimental results can be fitted satisfactorily by a straight line. The slope of the straight line is equivalent to the critical exponent,  $\beta$ . Sixteen measured data at the reduced temperature differences from 0.00013 to 0.025 were used for the determination of the critical exponent,  $\beta$ , and the critical amplitude,  $B$ , in the least-squares fitting. Their values are

$$\beta = 0.347 \pm 0.002 \quad B = 2.055 \pm 0.021$$

where the uncertainties are the standard deviations in the least-squares fitting. The  $\beta$  of HFC-134 is greater than the theoretical value of 0.325 (10).

On the basis of 14 present measurements above  $594 \text{ kg}\cdot\text{m}^{-3}$  in density and saturated liquid density data reported by Maezawa et al. (8), the following correlation was developed:

$$(\rho' - \rho_c) / \rho_c = 1.9266\tau^{0.347} + 2.8310\tau^{0.75} - 3.0117\tau^{0.85} + 1.0885\tau^{1.34} \quad (3)$$

where  $\tau = (T_c - T) / T_c$ ;  $T$  is temperature in Kelvin on ITS-90.

The first exponent in eq 3 is the critical exponent,  $\beta$ , while other exponents were determined by trial and error. The effective temperature range of eq 3 is from 200 K to the critical temperature. The deviation plots for the data by Tamatsu et al. (9) and the correlation developed by Maezawa et al. (8) from eq 3 are shown in Figure 4. Equation 3 reproduces this

data and the data by Maezawa et al. (8) with the standard deviations of  $\pm 0.31\%$  and  $\pm 0.11\%$ , respectively, while the data by Tamatsu et al. (9) shifted from eq 3 by about  $+0.4\%$ .

## Conclusion

By means of visual observation of the meniscus in the optical cell, 28 saturated vapor and liquid densities of HFC-134 in the critical region, the critical temperature, the critical density, and the critical exponent,  $\beta$ , were determined. A saturated liquid density correlation for HFC-134 was developed on the basis of the present measurements with other available liquid density data. Our correlation is able to reproduce our data and other available data in the range of temperatures from 200 K to the critical temperature within their reported uncertainties.

## Acknowledgment

We are indebted to Daikin Industries Ltd., Osaka, for kindly furnishing the samples. Kenichi Kishi and Seisho Tanikawa, who were former undergraduate and graduate students at Keio University, are gratefully acknowledged.

## Literature Cited

- (1) Higashi, Y.; Ashizawa, M.; Kabata, Y.; Majima, T.; Uematsu, M.; Watanabe, K. *JSME Int. J.* 1987, 30 (265), 1106.
- (2) Kabata, Y.; Tanikawa, S.; Uematsu, M.; Watanabe, K. *Int. J. Thermophys.* 1989, 10 (3), 605.
- (3) Tanikawa, S.; Kabata, Y.; Sato, H.; Watanabe, K. *J. Chem. Eng. Data* 1991, 35 (4), 381.
- (4) Tanikawa, S.; Tatoh, J.; Maezawa, Y.; Sato, H.; Watanabe, K. *J. Chem. Eng. Data* 1992, 37 (1), 74.
- (5) Okazaki, S.; Higashi, Y.; Takaishi, Y.; Uematsu, M.; Watanabe, K. *Rev. Sci. Instrum.* 1983, 54 (1), 21.
- (6) Higashi, Y.; Okazaki, S.; Takaishi, Y.; Uematsu, M.; Watanabe, K. *J. Chem. Eng. Data* 1984, 29 (1), 31.
- (7) Higashi, Y.; Uematsu, M.; Watanabe, K. *Trans. JSME* 1985, 28 (285/286), 2660.
- (8) Maezawa, Y.; Sato, H.; Watanabe, K. *J. Chem. Eng. Data* 1991, 36 (2), 151.
- (9) Tamatsu, T.; Sato, H.; Watanabe, K. *J. Chem. Eng. Data* 1992, 37 (2), 216.
- (10) Levelt Sengers, J. M. H.; Sengers, J. V. In *Perspectives in Statistical Physics*; Raveche, H. J., Ed.; North-Holland: Amsterdam, 1981; Chapter 14.

Received for review May 20, 1992. Accepted September 4, 1992.